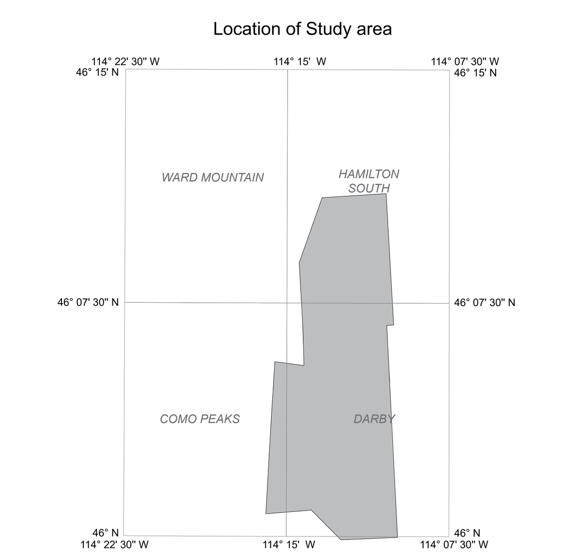

Shaded relief created from lidar and 10 meter digital elevation model from U.S. Geological Survey National Elevation Dataset.

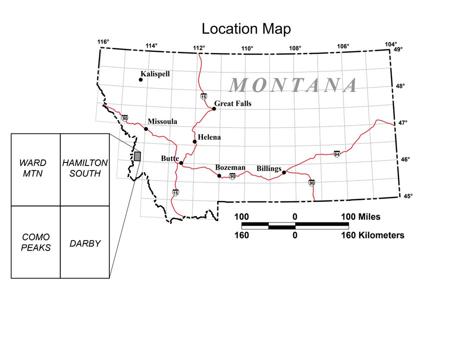

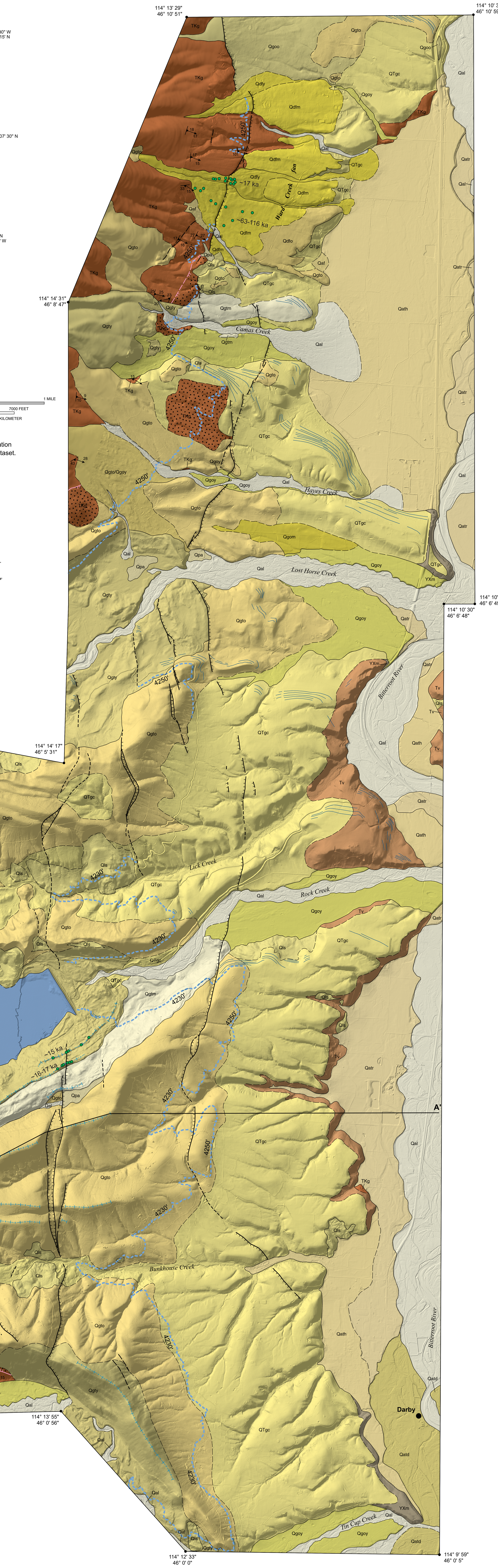

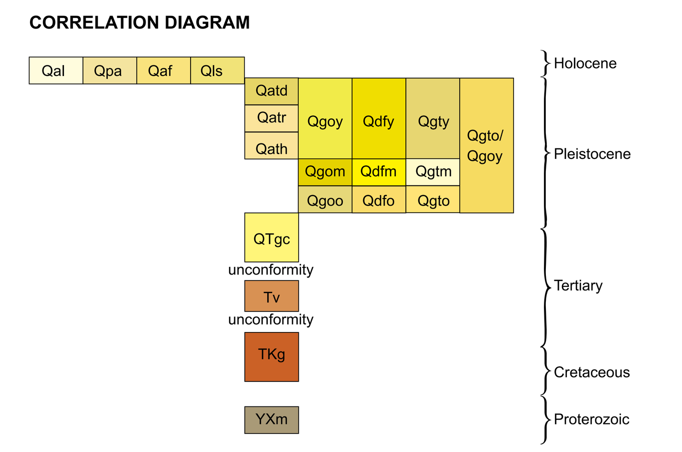

MAP SYMBOLS

- Contact: dashed where approximately located
- Fault: dashed where approximately located; dotted where concealed
- Detachment fault: hachures on upper plate; dashed where approximately located
- Scarp on fault: dashed where approximately located;hachures point downscarp
- Inclined metamorphic or tectonic foliation: showing strike and dip
- Approximate plunge direction of inclined lineation
- Geochron points
- Shoreline
- Glacial Moraine Crest
- 4230' Glacial Lake Missoula maximum elevation (only shown where mappable)
- Breccia

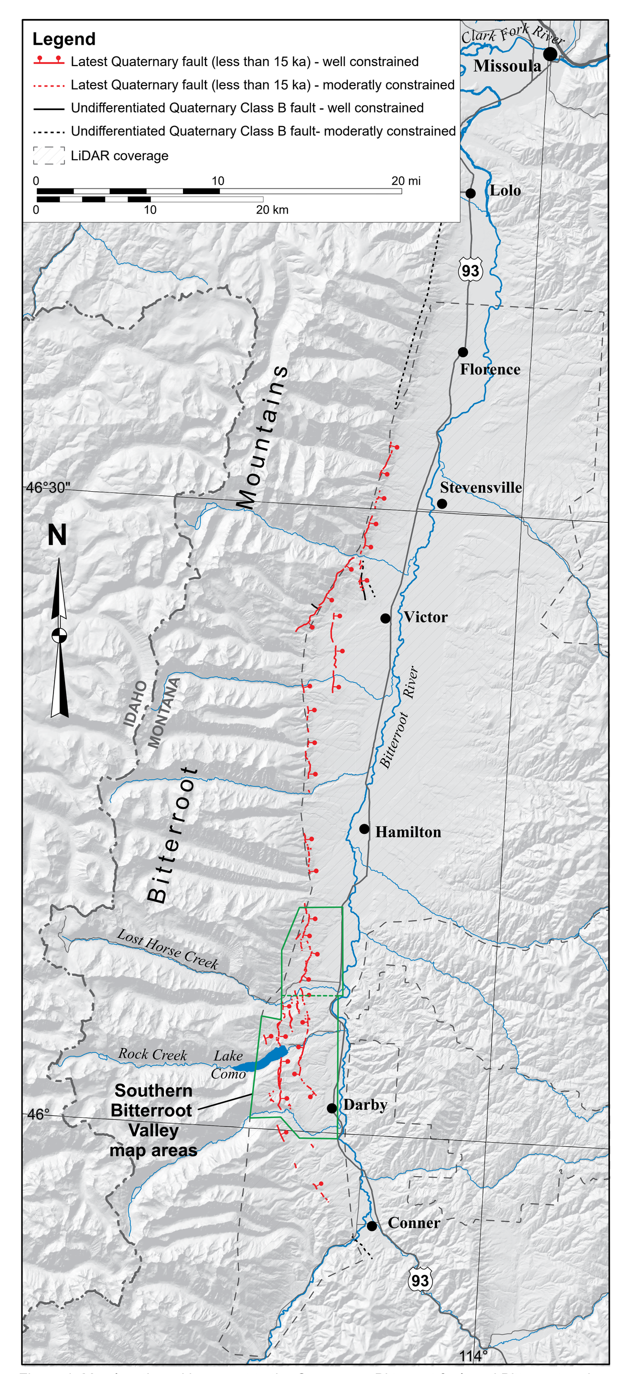

Figure 1. Map location with respect to the Quaternary Bitterroot fault and Bitterroot and Missoula valleys. Inset box (green outline) indicates location of new mapping from this study near Lake Como. Northern section of the new map (north of east-west dashed line in the inset box) indicates mapping revised from Stickney and Lonn (2018). Quaternary faults shown on regional map are derived from the Montana Quaternary Fault Database that includes new updates from this study and previous updates from the USGS Quaternary Fault and Fold Database.

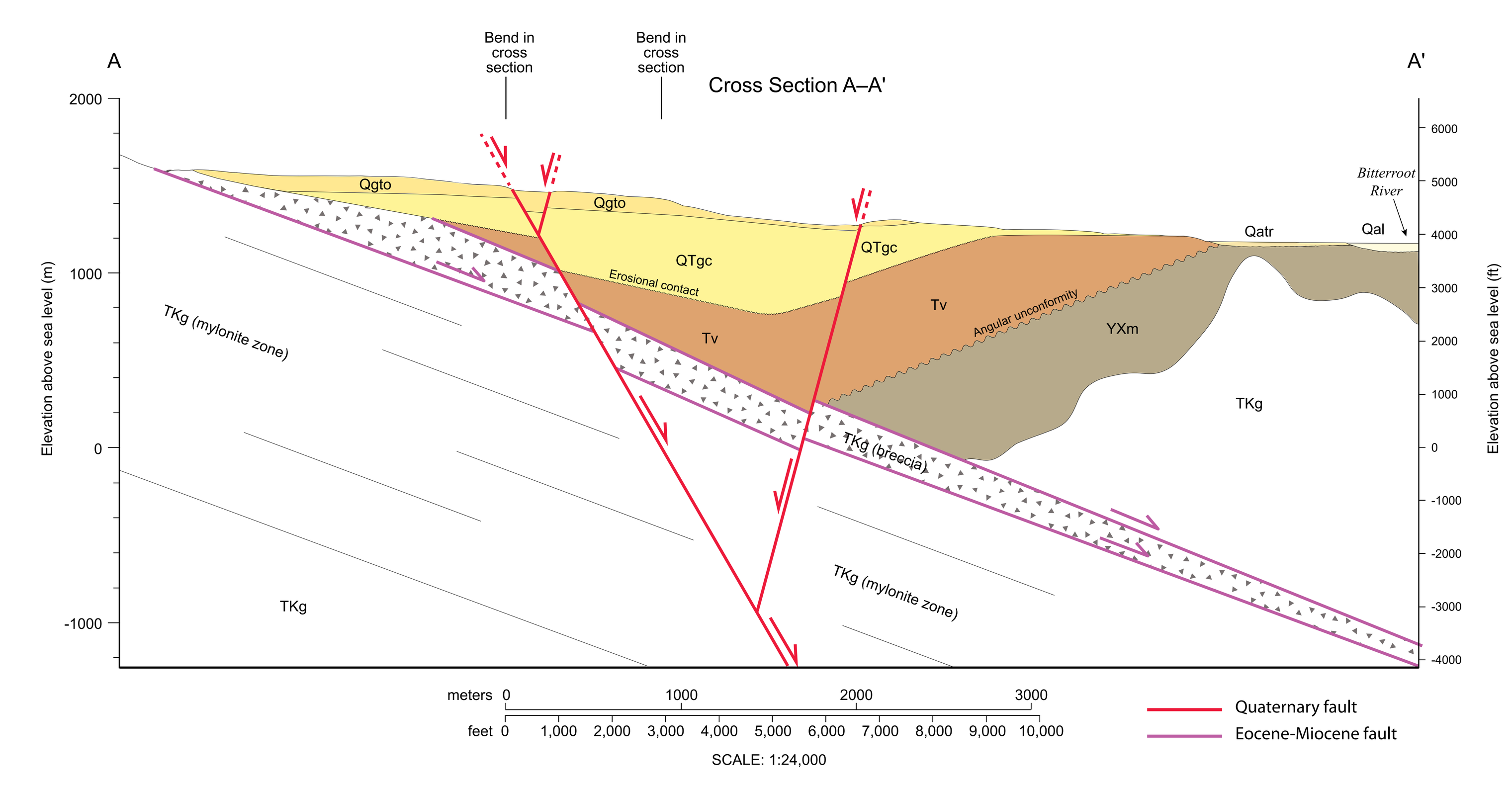

Introduction

This new 1:24,000 geologic map, encompassing 118 km^2 in the southern Bitterroot Valley of western Montana (fig. 1), was produced as part of a study characterizing Late Quaternary fault scarps and slip rates (Gavillot and others, 2021) on the recently recognized active Bitterroot fault. The Bitterroot fault is broadly categorized as a continuous north–south-trending normal fault with Quaternary activity that extends for ~100 km along the eastern Bitterroot Mountains range front (fig. 1). The Bitterroot fault is the primary seismogenic fault system with the potential to cause surface-rupturing earthquakes affecting the Missoula and Bitterroot Valleys. We chose this map area because previous mapping (Lonn and Sears, 2001; Stickney and Lonn, 2018) and lidar data demonstrate that numerous fault scarps offset Pleistocene–Holocene deposits and surfaces of various ages, offering the opportunity to constrain the late Quaternary fault history and determine slip rates for seismic source characterization. Mapping was combined with ^{10}Be cosmogenic radionuclides exposure dating and the new lidar data to accomplish these goals (Gavillot and others, 2021). The map builds on previous work in the Bitterroot Valley by Lonn and Sears (2001; scale 1:100,000) and Stickney and Lonn (2018; scale 1:12,000). It was partly funded by the U.S. Geological Survey (USGS), National Earthquake Hazards Reduction Program under USGS award number G20AP00047.

Previous Work

Small-scale maps by Ross (1952), Toth (1983), McMurtrey and others (1972), Berg and Lonn (1996), Lonn and Berg (1996), and Lonn and Sears (2001) cover both bedrock and surficial geology of the region. Weber (1972) studied the glacial history of the valley, and Barkman (1984) and Cartier (1984) addressed the question of active tectonism in the Bitterroot Valley. Stickney and Lonn (2018) included a 1:12,000-scale map of the northern part of this map area that was revised during this study.

Geological Setting

The Bitterroot Mountains on the west side of the map area comprise the metamorphic infrastructure of a well-studied Eocene metamorphic core complex (e.g., Hyndman, 1980; Foster and others, 2001). The gently east-dipping Eocene Bitterroot detachment fault (called the B-detachment herein to distinguish it from the Quaternary Bitterroot normal fault) was responsible for the exhumation of the footwall rocks from depths of >20 km (>12 mi) between 53 and 30 Ma (Foster and others, 2001). The footwall is comprised of Cretaceous to Eocene intrusive rocks (TKg) and less common Mesoproterozoic–Paleoproterozoic metamorphic rocks (YXm). The B-detachment exhibits a transition from amphibolite facies mylonitization to greenschist facies shearing to brittle faulting through time as structural levels became increasingly shallow. Early deep-level movement on the B-detachment produced a >500 m-thick (>1,500 ft-thick) zone of amphibolite-facies gneissic granite containing numerous thin mylonitic zones parallel to the layering and easily recognizable in the clasts that are incorporated into younger deposits. The mylonitic gneiss is relatively resistant to weathering, and forms the striking planar slope of the Bitterroot Mountain front. The hanging wall of the B-detachment is comprised mainly of Mesoproterozoic–Paleproterozoic metasedimentary rocks (YXm) with lesser Cretaceous to Eocene granitic rocks (TKg). Tertiary volcanic rocks (Tv) unconformably and discontinuously overlie the metamorphic–plutonic bedrock. McMurtrey and others (1972) obtained a few fossil plants from the Tv unit yielding somewhat equivocal ages (ranging from Paleocene to Miocene) and proposed Tv is most likely late Oligocene to early Miocene. In the few places where hanging wall rocks are preserved near the B-detachment, they are extensively brecciated, in contrast to the gneissic and mylonitized footwall rocks. On the map, the trace of the B-detachment fault is shown at the contact between the amphibolite facies mylonitic gneiss (TKg), shown by mylonitic foliation and lineation symbols, and the brecciated rocks. The trace of the B-detachment is exposed discontinuously near and along the mountain front in the map area.

Foster and Raza (2002) postulated that steep east-dipping normal faults in the Bitterroot Valley, such as the Bitterroot fault, were Miocene in age and responsible for the uplift and exposure of the older Eocene B-detachment fault. Stickney and Lonn (2018) postulated that post-Miocene erosion driven by uplift on the Bitterroot fault removed most of the brecciated and less resistant rocks of the B-detachment hanging wall, leaving the resistant gneiss of the footwall to form the planar, gently sloping Bitterroot Mountain front. However, no apatite fission track (AFT) cooling ages, and therefore exhumation, younger than ~22 Ma have been recorded along the range front (Foster and Raza, 2002). The lack of evidence for steep-sloping (>30°) range front facets or significant topographic relief across the Bitterroot fault contradicts a tectonically active landscape controlled by a Bitterroot fault active since early Miocene. Gavillot and others (2021) estimates of total fault displacement from cross sections are consistent with the interpretation of a young (Late Miocene to Pliocene/Pleistocene) onset for the Bitterroot fault. The extensive pediment surfaces developed in the map area that were subsequently offset by strands of the Bitterroot fault also argue for late onset of fault activity because pediments are more likely to develop in areas of tectonic stability (Dohrenwend and Parsons, 2009). The Bitterroot fault may represent the modern expression of Basin-and-Range-style extension in the Northern Rockies and maintains a high-angle normal fault geometry at depth (Cross Section A–A'). Alternatively, the Quaternary Bitterroot fault may represent a low-angle normal fault controlled at depth by the structural inheritance of the gentle-dipping Bitterroot detachment mylonitic gneiss (Gavillot and others, 2021).

Cenozoic Stratigraphy

An early Miocene minimum age for the Tv unit (see discussion above) raises the possibility that ancestral Bitterroot Valley deposits, as recorded in fluvial gravels within the QTgc map unit, may have resulted from exhumation by the Eocene B-detachment rather than the younger Bitterroot fault. While only late Miocene fossils have been found in QTgc (Konizeski, 1958; McMurtrey and others, 1972; Dale Hanson, Museum of the Rockies, written commun., 2018), it is possible that only the uppermost QTgc is currently exposed. QTgc accumulated to depths of at least as 700–1000 m (2300–3300 ft) north of Hamilton, based on well logs and gravity model constraints (Norbeck, 1980; Smith, 2006). QTgc consists of sandy, well-sorted, pebble–cobble conglomerate containing rounded clasts dominantly of Belt quartzite, but also including lesser granite, mylonitic gneiss, volcanic rocks, and metamorphic rocks. These fluvial gravels are interbedded with tuffaceous silt and clay intervals interpreted as floodplain deposits (Lonn and Sears, 2001). Because the clasts are derived from lithologies present in the entire Bitterroot River basin, Lonn and Sears (2001) interpreted QTgc as deposited by an ancestral Bitterroot River and its tributary streams and fans. Interfingering with these lithologies along both sides of the valley are debris flow deposits characterized by sub-angular boulders derived from the adjacent mountains (Stickney and Lonn, 2018; McMurtrey and others; 1972). These facies relationships suggest that both the Sapphire and Bitterroot Mountains had significant relief along the north–south-trending flanks of the Bitterroot Valley by at least late Miocene time, and possibly since the Oligocene.

At least three glacial advances are recorded by late Quaternary till and associated outwash and debris flow deposits (Weber, 1972; Stickney and Lonn, 2018). The older glacial deposits mantle or underlie relict pediment surfaces. Younger and middle-aged glacial till is nested within the older, more extensive moraines, and younger outwash and debris flow deposits are incised into the older glacial deposits.

The older glacial deposits may represent at least three glacial advances: we recognized three lateral moraine crests within older till (Qgto) south of Lake Como. Field observations (smooth and inflated surfaces), topographic positions, and ^{10}Be cosmogenic radionuclides exposure dates of 97–116 ka on the Ward Creek fan, a glacial debris fan with complex deposits located in the northern map area (Gavillot and others, 2021), suggest these older glacial moraines represent Bull Lake or older glaciation (>100 ka; Pierce, 2003 and references therein; Liccardi and Pierce, 2008).

In some areas, intermediate-level glacial deposits between the young deposits and older deposits were recognized, and are labeled as middle-aged on the map. An intermediate-level debris flow (Qdfm), probably emplaced during a glacial outburst flood on the Ward Creek fan, yielded ^{10}Be cosmogenic radionuclide ages of ~63–70 ka (Gavillot and others, 2021) and are interpreted to represent age of the middle-aged glacial deposits.

Numerous parallel moraine crests occur within younger till (Qgty) south of Lake Como and in the Lost Horse Creek area (fig. 1). ^{10}Be cosmogenic radionuclides exposure dating of two parallel lateral moraine crests within younger till (Qgty) south of Lake Como yielded ages of ~16–17 ka for the outer oldest Pinedale moraine and ~15 ka for the inner younger moraine (Gavillot and others, 2021). Similarly, dating of the youngest Ward Creek fan debris flow (Qdfy) yielded peak age distributions of ~16–17 ka (Gavillot and others, 2021). These young glacial deposits are interpreted to represent Pinedale Glaciation (~15–20 ka; Pierce, 2003 and references therein; Liccardi and Pierce, 2008).

Glacial Lake Missoula filled the valley at times to elevations as high as 4,250 ft (1,295 m) and left strand lines visible on the lidar and shown on the geologic map. These formed prior to 13.7–13.4 ka, the age of youngest Glacial Lake Missoula sediments (Smith and others, 2018), with high stand strand lines visible on the ~15 ka moraine at Lake Como, constraining their maximum age (Gavillot and others, 2021). The 4,250 ft (1,295 m) elevation high stand is shown where strand lines are visible at this elevation. In the Rock Creek area ~1.6 km (~1 mi) east of Lake Como, high stand shorelines are offset across a down-to-the-west fault scarp interpreted as an antithetic strand of the Bitterroot fault. High stand strand lines in the hanging wall on the west side of the fault have been dropped down to the 4,230 ft (1,289 m) elevation (Gavillot and others, 2021).

The youngest sedimentary deposits are the boulder- to cobble-gravels of modern streams (Qal), and organic material that built up in shallow lakes and marshes (Qpa). Landslides (Qls, Qlso) are commonly developed in areas underlain by clay-rich QTgc and Tv.

Pediment Surfaces

Pediment surfaces are common and extensive in the map area (fig. 2). The most obvious pediments are in the Ward Creek fan area and north of Hayes Creek, where parts of the surfaces are developed on granitic bedrock. Other well-developed pediments occur west of Darby, north of lower Lost Horse Creek, and north of Rock Creek (fig. 1). The Rock Creek pediment surface is offset by the down-west scarp of the antithetic fault strand. Other elevated, gently sloping, low-relief but less planar areas, are also interpreted as pediments that are less mature, more dissected, or covered by younger deposits (for example, surfaces south of upper Lost Horse Creek and north of Camas Creek). The pediments occur at several topographic levels and must be of several different ages. The pediment surfaces are not covered by transported alluvium, but instead appear to consist of the underlying material weathered in place. They are therefore classified as mantled rock pediments (Twidale, 2014) formed by an etching process. The pediments indiscriminately bevel mylonitic gneiss, brecciated granite, volcanic rocks, and QTgc. Parts of the Hayes Creek pediment appear to bevel glacial till; parts of the Ward Creek fan pediment are developed on glacial debris fan deposits; and most pediments include areas floored by uppermost QTgc, all suggesting a Quaternary age for some pediments. Larson and others (2016) showed that pediment surfaces in an area of rapidly changing base level formed within just one glacial-interglacial cycle, in as little as 50,000 years. The Bitterroot fault offsets several pediment surfaces, with vertical offsets ranging from 11 m (35 ft) on the Hayes Creek pediment to 14 m (47 ft) on the Ward Creek fan pediment, to as much as 43 m (141 ft) north of the map area near Victor (Stickney and Lonn, 2018). Absolute ages of these surfaces would be useful in determining slip rates, but are not yet available.

Quaternary Bitterroot fault

The geologic map shows that the Quaternary Bitterroot fault is expressed by numerous, parallel, *en echelon* fault scarps trending north–south to northwest–southeast. The majority of scarps show east-side-down vertical offset, but west-dipping faults and small grabens also occur (fig. 3). Map relations, field observations, and topographic and cross-section constraints indicate the main trace of the Bitterroot fault is an east-dipping 45–70°E normal fault that either continues as a high-angle fault at depth (cross section A–A'), or shallows into pre-existing weaknesses along the B-detachment (see Gavillot and others, 2021 for low-angle fault geometry). East of Lake Como and the main fault trace, mapping revealed a ~10 km-long west-dipping 70–80°W normal fault that is interpreted as an antithetic structure to the main strand of the east-dipping Bitterroot fault (cross section A–A', fig. 3C).

Fault scarps cut Quaternary glacial deposits of several ages as well as some pediment surfaces. Although few absolute ages are available, the amount of offset increases with the relative ages of the surface (Stickney and Lonn, 2018). Gavillot and others (2021) used ^{10}Be cosmogenic radionuclides exposure dates and measurements of vertical separation from two offset Pinedale moraines south of Lake Como and two offset debris fans on the Ward Creek fan to quantify average late Quaternary fault slip rates at 0.2–0.3 mm/yr (0.25 ± 0.05 mm/yr). Offset high-stand Lake Missoula strand lines yielded a slip rate of 0.2–0.4 mm/yr for the west-dipping antithethic normal fault east of Lake Como (Gavillot and others, 2021).

Description of Map Units

Qal **Stream alluvium (Holocene and Late Pleistocene)**—Subangular to rounded, moderately to well sorted and stratified, imbricated pebble to boulder sandy gravel deposited by modern streams. Gravel clasts are representative of individual drainage basins, and are dominated by granite, mylonitic granite, quartzite, and volcanic rocks. Includes flood plain deposits of sand, silt, and clay. Includes minor colluvium and alluvial fan deposits. Deposits are 1–18 m (3–60 ft) thick (McMurtrey and others, 1972).

Qpa **Paludal deposit (Holocene)**—Organic matter, sand, silt, and clay accumulated in swamps, marshes, ponds, and lakes. Thickness probably less than 5 m (16 ft).

Qaf **Alluvial fan and debris-flow deposits (Holocene and Late Pleistocene)**—Subangular to rounded, poorly sorted, matrix-supported pebble to boulder gravel in a sand, silt, and clay matrix. Commonly grades into, interfingers with, or caps stream alluvium (Qal). Thickness varies greatly, ranging from 1 to 24 m (3–75 ft).

Qls **Landslide and earthflow deposits (Holocene and late Pleistocene)**—Unsorted and unstratified mixtures of locally derived mass movement deposits transported down adjacent slopes and characterized by irregular hummocky surfaces. Occurs most commonly as earthflows on slopes underlain by Tv or clay-rich facies of the ancestral Bitterroot River deposits (QTgc).

Qatd **Alluvium of the Darby terrace (late Pleistocene?)**—The youngest and lowest Bitterroot River strath terrace, underlying most of the town of Darby. Bevels QTgc but probably includes a thin veneer of late Quaternary alluvium estimated to be 1–3 m (3–10 ft) thick. The late Quaternary alluvium and QTgc are difficult to distinguish because of their nearly identical lithologies. Well-rounded, well-sorted gravel and sand with predominantly granitic, gneissic, Belt metasedimentary, and minor volcanic clasts. The Darby terrace surface stands 2–3 m (6–10 ft) above the modern Bitterroot River floodplain.

Qatr **Alluvium of the Riverside terrace (late Pleistocene?)**—The second youngest Bitterroot River strath terrace, termed the Riverside terrace by Weber (1972). Bevels QTgc but probably includes a thin veneer of late Quaternary alluvium estimated to be 1–3 m (3–10 ft) thick. The late Quaternary alluvium and QTgc are difficult to distinguish because of their nearly identical lithologies. Well-rounded, well-sorted gravel and sand with predominantly granitic, gneissic, Belt metasedimentary, and minor volcanic clasts. The Riverside terrace surfaces stand 3–5 m (10–16 ft) above the modern Bitterroot River floodplain.

Qath **Alluvium of the Hamilton terrace (late Pleistocene?)**—The oldest recognized Bitterroot River strath terrace, named the Hamilton terrace by Weber (1972). Bevels QTgc but probably includes a thin veneer of late Quaternary alluvium estimated to be 1–3 m (3–10 ft) thick. The late Quaternary alluvium and QTgc are difficult to distinguish because of their nearly identical lithologies. Well-rounded, well-sorted gravel and sand with predominantly granitic, gneissic, Belt metasedimentary, and minor volcanic clasts. Hamilton terrace surfaces stand 6–8 m (20–26 ft) above the modern Bitterroot River floodplain.

Qgto/oy **Younger glacial outwash deposits and older glacial till deposits, undivided (Pleistocene)**—Mapped south of Hayes Creek, where older glacial till underlying the Hayes Creek pediment surface was eroded by meltwater from Pinedale glaciers that also deposited younger bouldery outwash gravels. Characterized by a gently undulating surface containing scattered, enormous, angular gneissic and granitic boulders that are badly weathered, and abundant, fresher, well-rounded cobbles and boulders.

Qgoy **Younger glacial outwash deposits (latest Pleistocene to early Holocene)**—Subrounded to well-rounded, moderately to well-sorted, unweathered cobbles and boulders in a matrix of sand and gravel deposited in outwash fans downstream from Pinedale-age glaciers. Surfaces of these deposits are at a lower level than older outwash (Qgoo and Qgom) and 2–8 m (7–26 ft) above active channels and stream deposits (Qal). Can be traced upstream to Pinedale glacial till deposits (Qgty) and is likely similar in age or younger. Some fans appear to coalesce with alluvial terrace deposits (Qatr and Qath). Thickness averages 12 m (39 ft) (McMurtrey and others, 1972).

Qgty **Younger glacial till deposits (late Pleistocene)**—Unsorted, mostly unstratified, clay, silt, sand, and gravel containing boulders up to 6 m (20 ft) in diameter. Clasts subangular to subrounded and unweathered. Characterized by very hummocky appearance on the lidar image. Deposited in Pinedale-age glacial moraines typically inset within older moraines (Qgto and Qgtm). Within the Pinedale deposits (Qgty) south of Lake Como are several parallel, inset moraine crests of slightly different ages. ^{10}Be cosmogenic radionuclides exposure dating of two parallel lateral moraine crests yielded ages of ~16–17 ka for the outer oldest Pinedale moraine and ~15 ka for the inner, younger moraine (Gavillot and others, 2021). There appear to be other, younger parallel lateral moraines (not shown on map) inset within the ~15 ka moraine in Qgty. Thickness probably ranges from 10–120 m (33–400 ft).

Qdfy **Younger glacial debris flow deposits (latest Pleistocene to early Holocene)**—Subangular to well- rounded, poorly sorted, matrix-supported, unweathered boulders and cobbles in a matrix of sand, gravel, and clay. Characterized by boulders as much as 3 m (10 ft) in diameter, and by a hummocky appearance on the lidar image. Deposited in debris-flow fans below Pinedale-age glaciers, probably as a result of catastrophic glacial outburst floods. Good exposures occur on the Ward Creek fan, where the upstream ends overlie a bedrock pediment surface and the downstream ends are incised into the pediment surface. 10Be cosmogenic radionuclides exposure dating of the Ward Creek Qdfy yielded peak age distributions of ~16–17 ka (Gavillot and others, 2021). Thickness probably 2–12 m (7–39 ft).

Qgom **Middle-aged glacial outwash deposits (Pleistocene)**—Subrounded to well-rounded, moderately sorted, unweathered cobbles and boulders in a matrix of sand and gravel deposited in outwash fans downstream from Pleistocene glaciers. Surfaces of these deposits stand at an intermediate level between younger and older glacial outwash (Qgoy and Qgoo), but their absolute ages are unknown. Some can be traced upstream to middle-aged glacial till deposits (Qgtm). Thickness probably 2–12 m (7–39 ft).

Qgtm **Middle-aged glacial till deposits (Pleistocene)**—Unsorted, mostly unstratified, clay, silt, sand, and gravel containing boulders up to 6 m (20 ft) in diameter. Clasts subangular to subrounded and variably weathered. Deposited in Pleistocene glacial moraines. Characterized by their smooth surfaces on the lidar image in contrast to younger till (Qgty) with well-preserved hummocky topography. Distinguished where intermediate-aged moraines can be identified between the Pinedale moraines (Qgty) and older moraines (Qgto). In other areas, they could not be distinguished from Qgto and are included in Qgto. Thickness ranges from 10–120 m (33–400 ft).

Qdfm **Middle-aged glacial debris flow deposits (late Pleistocene)**—Subangular to well-rounded, poorly sorted, matrix-supported, unweathered boulders and cobbles in a matrix of sand, gravel, and clay. Characterized by boulders as much as 3 m (10 ft) in diameter, and by a hummocky appearance on the lidar image. Deposited in debris-flow fans, probably as a result of catastrophic glacial outburst floods. Surfaces of these deposits stand at an intermediate level between younger and older glacial outwash (Qgoy and Qgoo) and debris flows (Qdfy and Qdfo). Good exposure occurs on the Ward Creek fan. ^{10}Be cosmogenic radionuclides exposure dating of the Ward Creek Qdfm yielded peak age distributions of ~63–70 ka (Gavillot and others, 2021), possibly correlating to Marine Isotope Stage 4 (MIS 4) or Early Wisconsin Glaciation (~60–70 ka). A secondary older boulder age population in Qdfm of 97–116 ka may represent exposure inheritance from Qdfo, representing Marine Isotope Stage 6 (MIS 6) or Bull Lake Glaciation (>100 ka) (Pierce, 2003 and references therein; Liccardi and Pierce, 2008). Thickness probably 2–12 m (7–39 ft).

Qgoo **Older glacial outwash deposits (Pleistocene)**—Subrounded to well-rounded, moderately sorted, variably weathered cobbles and boulders in a matrix of sand and gravel deposited in outwash fans downstream from Pleistocene glaciers. Surfaces of these deposits lie above the younger outwash fans (Qgoy and Qgom). Mapped as Tertiary Sixmile Creek Formation on Lonn and Sears (2001), but reassigned to a Pleistocene age herein because they can be traced upstream to older glacial moraines (Qgto). Thickness from 2–12 m (7–39 ft).

Qgto **Older glacial till deposits (Pleistocene)**—Unsorted, mostly unstratified, clay, silt, sand, and gravel containing boulders up to 6 m (20 ft) in diameter. Clasts subangular to subrounded and variably weathered. Deposited in older Pleistocene glacial moraines, possibly of Bull Lake age and older. Characterized by their smooth surfaces on the lidar image in contrast to younger till (Qgty). Also mapped underlying parts of the Hayes Creek pediment surface. Weber (1972) postulated that at least two different glacial stages are represented by these deposits, but we could not distinguish them in the field or on the lidar image except south of Lake Como where at least two lateral moraine crests are preserved and included in Qgto. Thickness ranges from 10–120 m (33–400 ft).

Qdfo **Older glacial debris flow deposits (Pleistocene)**—Subangular to well-rounded, poorly sorted, matrix-supported, variably weathered boulders and cobbles in a matrix of sand, gravel, and clay. Characterized by boulders as much as 3 m (10 ft) in diameter, and by a slightly hummocky appearance on the lidar image. Deposited in debris-flow fans below Pleistocene glaciers, probably as a result of catastrophic glacial outburst floods. Appears to underlie part of the Ward Creek fan pediment surface, but may also mantle pediments developed on the ancestral Bitterroot River deposits (QTgc). Some were mapped as Tertiary Sixmile Creek Formation by Lonn and Sears (2001), but reassigned to a Pleistocene age herein because they can be traced upstream to older glacial moraines (Qgto). Thickness ranges from 12 m (39 ft) at the heads of fans to less than 2 m (7 ft) near the toes.

QTgc **Gravel and clay of the ancestral Bitterroot River deposits (Oligocene to Plio-Pleistocene?)**—Unconsolidated, moderately to well-sorted, stratified, sub-angular to well-rounded, fluvial gravel and sand interbedded with light tan clay, silt, and tephra. Deposited in channels and floodplains of the ancestral Bitterroot River (Lonn and Sears, 2001) and tributary streams and fans. Gravel deposits commonly contain well-rounded cobbles and pebbles of (in order of decreasing abundance): Belt quartzite, granite/granodiorite, mylonitic gneiss, high-grade metamorphic rocks, and extrusive volcanic rocks that represent rocks exposed in the entire Bitterroot River drainage. Interbedded finer grained deposits, probably deposited in adjacent floodplains, are light gray clay and silt deposits in beds 15 cm (6 in) to 1.5 m (5 ft) thick, with abundant interbedded tephra. Some brown, ledge-forming massive silty layers with root casts and burrows are present and interpreted to be paleosols. Westward and stratigraphically upward, gravel becomes dominated by granitic and mylonitic gneiss clasts (fig. 3C); these are generally well-rounded near the valley center, and are well-rounded to sub-angular, and sometimes bouldery, near the western valley's western edge. A 60 m (200 ft) thickness of granite-dominated gravel is exposed along the road 1.6 km (1 mi) east of Como Dam. It is unclear whether these upper granitic gravels are Quaternary or Tertiary in age, or both. Some underlie the pediment surfaces described above, while others could have been deposited on top of pediment surfaces. The surface of the granitic gravel adjacent to the moraines west of Darby appears to have a steeper slope than the pediment, and so could be younger. However, these were not divided on the map due to the difficulty in distinguishing them. The upward increase in granitic clasts may represent the unroofing of the Bitterroot Mountains as incision proceeded into the granitic/gneissic footwall of the B-detachment. Lonn and Sears (2001) mapped most granitic-clast-dominated gravels as late Tertiary Sixmile Creek Formation, but they have been reassigned as Tertiary to Quaternary in this study due to the uncertainties described above. Fossils collected (McMurtrey and others, 1972; Konezeski, 1958; Dale Hanson, Museum of the Rockies, written commun. 2018) were all late Miocene (Clarendonian) in age. Although deep drill holes show that unconsolidated sedimentary rocks similar to QTgc are up to 700 m (2,300 ft) thick in places (Norbeck, 1980) in the central part of the valley north of the Como study area, maximum exposed thickness in the map area is about 100 m (330 ft). Lower contact is an unconformity with underlying Tv, TKg, and YXm; the lower depositional paleosurface appears to have had considerable relief. Upper contact is most often an erosional (pediment) surface, in some places overlain by Quaternary glacial till, such as the Lake Como area and in the valley of Bunkhouse Creek west of Darby.

Tv **Volcanic rocks (Paleocene to Miocene?)**—Rhyolite tuff and andesite flows. Mostly white to light gray to yellow-gray porphyritic latite tuff, red to pink rhyodacite vitrophyre, and volcanic breccia containing fragments of porphyritic basalt, rhyodacite, obsidian, and quartz latite. Includes interbedded volcanoclastic sedimentary beds. Plant fossils obtained (McMurtrey and others, 1972) indicate a Paleocene to Miocene age and Tv is thought to be related to extension associated with the B-detachment fault. Extensively exposed in the southeastern part of the map area in the bluffs west of the Bitterroot River. When Lake Como was at low levels, an outcrop of tuffaceous Tv was observed in the toe of a landslide on the north shore of Lake Como beneath normal pool elevation. Tuffaceous Tv is also exposed in a landslide scarp on the north side of Lick Creek, 1.6 km (1 mi) northeast of the Como Dam. Lower contact is an unconformity developed on units TKg and YXm. The lower contact with YXm is exposed in the map area in the large road cut along US 93 1 km south of the mouth of Lost Horse Creek (fig. 1). Upper contact is an unconformity with overlying QTgc. Thickness unknown.

TKg **Foliated granodiorite and unfoliated granite, undivided (Cretaceous and Eocene)**—In the footwall of the Bitterroot detachment, unit is weakly foliated to gneissic Cretaceous to Eocene biotite–muscovite granodiorite intruded by unfoliated Eocene biotite–muscovite granite. Fabrics in the granodiorite developed at deep levels early in the Bitterroot detachment fault's history, while the Eocene granite intruded at shallower levels following most of the plastic deformation. TKg in the B-detachment footwall contains numerous thin mylonitic zones parallel to the gneissic layering. In the B-detachment hanging wall, both unfoliated Eocene biotite-muscovite granite and weakly foliated to unfoliated biotite–muscovite granodiorite occur. A thick brecciated zone (as much as ~100–300 m thick) occurs immediately above the B-detachment, and grades upward into unbrecciated rocks. TKg also includes outcrop-scale inclusions of Belt metasedimentary rock that are too small to show on the map.

YXm **Metamorphic rocks (Proterozoic)**—Quartzite, amphibolite, and calc-silicate gneiss continuous with the metamorphic rocks of Sleeping Child Creek in the Sapphire Mountains in the hanging wall of the Bitterroot detachment. Includes numerous small Cretaceous-Tertiary granitic intrusions (larger, mappable intrusions are mapped as TKg). The Sleeping Child metamorphic rocks are comprised of 1860 Ma orthogneiss and >1378 Ma migmatitic quartzite with a Belt Supergroup protolith (Lonn and Mosolf, 2020) that were metamorphosed in Cretaceous–Tertiary time by voluminous granitic plutons.

References

Barkman, P.E., 1984, A reconnaissance investigation of active tectonism in the Bitterroot Valley, western Montana: M.S. thesis, Missoula, University of Montana, 85 p.
Berg, R.B., and Lonn, J.D., 1996, Preliminary geologic map of the Nez Perce Pass 30 x 60-minute quadrangle: Montana Bureau of Mines and Geology Open-File Report 339, scale 1:100,000.
Cartier, K.D.W., 1984, Sediment, channel morphology, and streamflow characteristics of the Bitterroot River drainage basin, southwestern Montana: M.S. thesis., Missoula, University of Montana, 191 p.
Dohrenwend, J.C., and Parsons, A.J., 2009, Pediments in arid environments, in Abrahams, A.D., and Parsons, A.J., eds., Geomorphology of desert environments, 2nd ed.: Springer, New York, p. 377–411, doi: http://dx.oi.org/10.1007/978-1-4020-5719-9_13.
Foster, D.A., Schaferb, C., Fanning, C.M., and Hyndman, D.W., 2001, Relationships between crustal partial melting, plutonism, orogeny, and exhumation: Idaho–Bitterroot batholith: Tectonophysics, v. 342, p. 313–350.
Foster, D.A., and Raza, A., 2002, Low-temperature thermochronological record of exhumation of the Bitterroot metamorphic core complex, northern Cordilleran Orogen: Tectonophysics, v. 349, no. 1–4, p. 23–36.
Gavillot, Y., Lonn, J., and Stickney, M., 2021, Quaternary slip rates and most recent surface rupture of the Bitterroot Fault, western Montana, from Cosmogenic radio nuclide dates of offset glacial deposits: U.S. Geological Survey, Earthquake Hazards Reduction Program Award Number, Final Technical Report G20AP00047, available at https://earthquake.usgs.gov/cfusion/external_grants/reports/G20AP00047.pdf [Accessed September 2022].
Hyndman, D.W., 1980. Bitterroot dome–Sapphire tectonic block, an example of a plutonic core–gneiss–dome complex with its detached suprastructure, in Crittenden, M.D., Coney, P.J., and Davis, G.H., eds., Cordilleran Metamorphic core complexes: Geological Society of America Memoir, v. 153, p. 427– 443.
Konizeski, R.L., 1958, Pliocene vertebrate fauna from the Bitterroot Valley, Montana, and its stratigraphic significance, Geological Society of America Bulletin 69, p. 325–345.
Larson, P.H., Kelley, S.B., Dorn, R.I., and Seong, Y.B., 2016, Pace of landscape change and pediment development in the northeastern Sonoran Desert, United States: Annals of the American Association of Geographers, v. 106, no. 6, p. 1195–1216.
Licciardi, J.M., and Pierce, K.L., 2008, Cosmogenic exposure-age chronologies of Pinedale and Bull Lake glaciations in greater Yellowstone and the Teton Range, USA: Quaternary Science Reviews, v. 27, no. 7–8, p. 814–831.
Lonn, J.D., and Berg, R.B., 1996, Preliminary geologic map of the Hamilton 30 x 60-minute quadrangle, Montana: Montana Bureau of Mines and Geology Open-File Report 340, scale 1:100,000.
Lonn, J.D., and Mosolf, J., 2020, Field guide to the geology of the Sleeping Child metamorphic complex, southern Sapphire Mountains, western Montana: Northwest Geology, v. 45, p. 35–56.
Lonn, J.D., and Sears, J.W., 2001, Geology of the Bitterroot Valley, shaded relief: Montana Bureau of Mines and Geology Open-File Report 441-C, 1 sheet, scale 1:48,000.
McMurtrey, R.G., Konizeski R.L., Johnson, M.V., and Bartells, J.H., 1972, Geology and water resources of the Bitterroot Valley, southwestern Montana. U.S. Geological Survey Water Supply Paper 1889, 80 p. scale 1:125,000.
Norbeck, P.M., 1980, Preliminary evaluation of deep aquifers in the Bitterroot and Missoula valleys in western Montana: Montana Bureau of Mines and Geology Open File Report 46, 15 p.
Pierce, K.L., 2003, Pleistocene glaciations of the Rocky Mountains, developments in Quaternary Sciences: San Diego, Elsevier, v. 1, p. 63–76.
Ross, C.P., 1952, The eastern front of the Bitterroot Range, Montana: U.S. Geological Survey Bulletin 974, p. 135–175, scale 1:125,000.
Smith, L., 2006, Altitude of the bedrock surface in the Bitterroot Valley: Missoula and Ravalli Counties, Montana: Montana Bureau of Mines and Geology Montana Ground-Water Assessment Atlas 4, part B, map 5.
Smith, L., Sohbati, R., Buylaert, J-P., Lian, O.B., Murray, A., Jain, M., 2018, Timing of lake-level changes for a deep last-glacial Lake Missoula: Optical dating of the Garden Gulch area, Montana, USA: Quaternary Science Reviews, v. 183, p. 23–35.
Stickney, M.C., and Lonn, J.D., 2018, Investigation of late Quaternary Fault scarps along the Bitterroot Fault in western Montana: Montana Bureau of Mines and Geology Report of Investigation 24, 16 p., 2 plates.
Toth, M.I., 1983, Reconnaissance geologic map of the Selway-Bitterroot Wilderness, Idaho County, Idaho, and Missoula and Ravalli Counties, Montana: U.S. Geological Survey Miscellaneous Field Studies Map MF-1495B, scale 1:125,000.
Twidale, C.R., 2014, Pediments and platforms: Problems and solutions: Geomorphologie, v. 20, p. 3–56, doi: https://doi.org/10.4000/geomorphologie.10480.
U.S. Geological Survey and Montana Bureau of Mines and Geology, 2006, Quaternary fault and fold database for the United States, available at http//earthquake.usgs.gov/hazards/qfaults/ [Accessed April 2018].
Weber, W.M., 1972, Correlation of Pleistocene glaciation in the Bitterroot Range, Montana, with fluctuations of Glacial Lake Missoula: Montana Bureau of Mines and Geology Memoir 42, 42 p.

Acknowledgments.
This material is based upon work supported by the U.S. Geological Survey under Grant No. G20AP00047 and received financial support from the Montana Bureau of Mines and Geology (MBMG). Thoughtful and constructive reviews from James Sears, Michael Stickney, and Katie McDonald helped improve this map publication. We would like to particularly thank Michael Stickney for his broader collaborating effort and assistance on the Bitterroot fault.

GIS production: Yiwen Li and Yann Gavillot, MBMG. Map layout: Susan Smith, MBMG. Editing: Susan Barth, MBMG.

Figure 2. Westward view of a pediment that extends south from Rock Creek to west of Darby. Open bench in middle ground is pediment developed on Tv and QTgc. Forested hills beyond are glacial moraines of various ages deposited by glaciers occupying the Rock Creek valley that holds Lake Como (in upper right). High mountains in background are TKg of the Bitterroot detachment footwall.

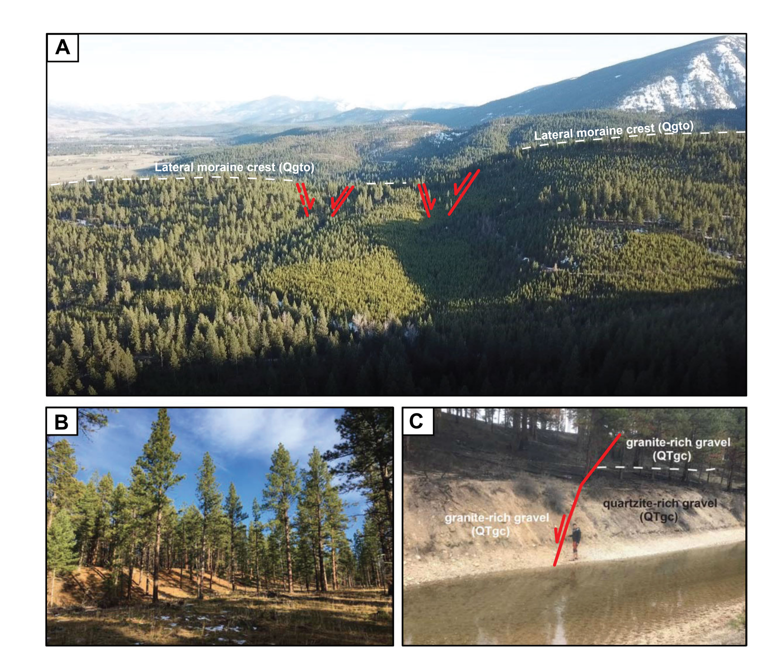

Figure 3. Photos of Bitterroot fault scarps. A) Southward view shows gentle (~20–30°) east sloping range front of the Bitterroot Mountains in the background, controlled by the B-detachment mylonitic gneiss. In the foreground are the high angle fault scarps (red lines) that offset old glacial moraine deposits (Qgto) with a fault scarp height of ~75 m (~250 ft). B) Northwest view of well exposed ~10m (33ft)-high fault scarp offsetting Qdfm, a middle-aged, ~63–70 ka (Gavillot and others, 2021) glacial debris fan surface on the Ward Creek fan. C) Northeast view of an outcrop exposure of the west-dipping antithetic fault near Rock Creek truncating deposits within the Quaternary-Tertiary gravels (QTgc). Note that granite-rich boulder gravel overlying quartzite-rich cobble gravel in the footwall on the right has been down-dropped in the hanging wall on the left (person for scale). Surface visible on skyline is a pediment surface that has also been offset by the fault.

Montana Bureau of Mines and Geology

Geologic Map 83

Geologic Map of the Southern Bitterroot Fault, Bitterroot Valley, Western Montana

Jeffrey D. Lonn and Yann G. Gavillot
2022

https://doi.org/10.59691/CBLY9091

Maps may be obtained from:
Publications Office
Montana Bureau of Mines and Geology
1300 West Park Street
Butte, Montana 59701-8997
Phone: (406) 496-4167
http://mbmg.mtech.edu